Vaccine 38 (2020) 6839–6848

Contents lists available at ScienceDirect

Vaccine

journal homepage: www.elsevier.com/locate/vaccine

VaxiPatch™, a novel vaccination system comprised of subunit antigens, adjuvants and microneedle skin delivery: An application to influenza B/Colorado/06/2017

Thomas J. Ellison, George C. Talbott, Daniel R. Henderson *

Verndari Inc., 2700 Stockton, Blvd, Suite 1104, Sacramento, CA 95817, United States

ARTICLE INFO

Article history:
Received 13 May 2020
Received in revised form 12 July 2020
Accepted 18 July 2020
Available online 31 July 2020

Keywords:
VaxiPatch™
Influenza virus rHA subunit antigen
QS-21 and PHAD adjuvants
Microneedle array
Point-of care vaccination

ABSTRACT

This work introduces VaxiPatch, a novel vaccination system comprised of subunit glycoprotein vaccine antigens, adjuvants and dermal delivery. For this study, rHA of influenza virus B/Colorado/06/2017 was incorporated into synthetic virosomes, and adjuvant liposomes were formed with QS-21 from *Saponaria quillaja*, with or without the synthetic TLR4 agonist 3D - (6-acyl) PHAD. These components were concentrated and co-formulated into trehalose with dye. Dermal delivery was achieved using an economical 37-point stainless steel microneedle array, designed for automated fill/finish by microfluidic dispensers used for mass production of immunodiagnostics. Vaccine and adjuvant are deposited to form a sugar glass in a pocket on the side of each of the tips, allowing skin penetration to be performed directly by the rigid steel structure. In this study, Sprague Dawley rats (n = 6 per group) were vaccinated by VaxiPatches containing 0.3 μg of rHA, 0.5 μg QS-21 and 0.2 μg 3D - (6-acyl) PHAD and dye, resulting in antigen-specific IgG titers 100-fold higher than 4.5 μg of FluBlok (p = 0.001) delivered intramuscularly. Similarly, hemagglutination inhibition titers in these animals were 14-fold higher than FluBlok controls (p = 0.01). Non-adjuvanted VaxiPatches were also compared with rHA virosomes injected intramuscularly. Accelerated shelf life studies further suggest that formulated virosomal antigens retain activity for at least two months at 60° C. Further, co-formulation of a dye could provide a visible verification of delivery based on the temporary pattern on the skin. A room-temperature-stable vaccination kit such as VaxiPatch has the potential to increase vaccine use and compliance globally.

1. Introduction

Vaccination is widely regarded as the most cost-effective form of medicine [1,2]. But we chronically under invest in them. Starting with the influenza vaccine introduced in 1945 vaccines have generally been lyophilized products to be reconstituted with water or saline, and delivered by intramuscular injection (IM) [3]. Vaccines as prefilled liquid syringes have become available. However, intradermal (ID) injection has long been known to offer advantages. ID injection was shown to only require 1/10th the dose of the IM influenza vaccine in the 1950s, and ID injection of inactivated polio virus (IPV) required 1/5th the dose of IM in 1953 [4]. Only Denmark adopted ID injection of IPV in the 1950s, a practice continued to this day [5]. Similarly, India has approved ID delivery of the rabies vaccine at 1/5th the dose to conserve vaccine supply. However, ID injections are more technically demanding than the traditional IM injection.

To reduce public resistance to vaccination, as demonstrated by the 2014 measles outbreak in California, improvements in vaccination procedures can be made [6]. Microarray skin patch vaccines hold the promise of painless delivery, circumventing fear of injection [7]. Fully 20% of the US adult population will not take a vaccine or even seek medical attention due to needle phobia [8]. Painless delivery could increase vaccine acceptance and use. In addition, microneedle skin patch vaccines can reduce the cost of vaccination. The potential cost reductions include: (a) eliminating or reducing dependency on the cold chain, (b) reducing of the vaccine active pharmaceutical ingredient (API) needed, and (c) the potential for self-administration of vaccines eliminating the need for expensive medical professionals. As recognized by BARDA, simplified administration and distribution of microneedle delivered vaccines also has the potential to accelerate the global response to pandemics threatened by infectious agents such as influenza, Ebola and SARS-CoV-2, the causative agent of COVID19.

* Corresponding author.
E-mail addresses: tellison@verndariinc.com (T.J. Ellison), gtalbott@verndariinc.com (G.C. Talbott), dhenderson@verndariinc.com (D.R. Henderson).

https://doi.org/10.1016/j.vaccine.2020.07.040
0264-410X/

Vaccines delivered by recently developed microneedle formats have been successful in both animal experiments and clinical trials [9–11]. However, these technologies have not yet offered manufacturing methods compatible with the high-volume and low-cost production requirements necessary to meet global needs. Metal microneedle formats have relied on a multiple dipping technique to achieve sufficient API loading, a technique which is poorly suited to efficient mass production [12]. A recent review of vaccines to be considered for skin microneedle delivery pointed out the needs in the field and focused on the vaccine needs for the Lower-and-Middle Income Countries (LMICs) MI [13]. Current dissolvable microneedle technologies require prohibitive inputs of labor and time to produce GMP compliant products [14–16]. By contrast, automated microfluidic dispensing technology has been used for over 15 years in the GMP manufacturing of Point-of-Care Immunodiagnostics, enabled by technologies from companies such as BioDot (Irvine, CA). Recent microarray vaccine efforts have focused on using existing approved vaccines such as those identified by PATH, including measles, rubella, HPV and rabies. The goal is fulfilling the vaccine needs of the lower-and-middle-income countries (LMICs) focusing on eliminating the cold chain, the need for reconstitution of lyophilized components, elimination of the sharps waste disposal and the waste associated with multi-dose vial packaging (PATH and Harro Hoefliger MAP Manufacturing Workshop, January 15–17, 2020, Allmersback im Tal, Germany) [13].

However, focusing only on dermal delivery of pre-existing FDA or EU approved vaccines significantly underestimates the need and the opportunity. Using microarray technologies, we can produce better vaccines at lower cost; vaccines that are more user-friendly that will result in higher levels of vaccine compliance. For example, subunit vaccines are safer than live-attenuated vaccines and easier to use in immunocompromised patients [17]. FluBlok, the only recombinant influenza vaccine on the market currently, has a higher efficacy than traditional inactivated influenza vaccines, but is given at three times the dose [18]. With the use of AS01-like adjuvants, seroconversion rates can be increased not only as shown for Shingrix® but across several vaccines and potentially in all age groups [19,20]. A cell phone photograph emailed to a healthcare provider of the dye pattern created by the microneedle administration of vaccines can provide proof of vaccination enabling self-administration of vaccines. The layout of microneedle arrays can be easily altered so that the dye transferred to the skin can create a transient "happy face" tattoo for childhood vaccines. Could this make vaccination enjoyable and even desired? Such vaccines are needed in both the LMICs and the higher-income countries (HICs).

This communication introduces VaxiPatch, a vaccination system that incorporates novel formulations of glycoprotein subunit vaccines, novel formulations of adjuvants and a novel microneedle array skin patch. As described here, subunit vaccines are produced by recombinant DNA methods in CHO or 293 cells and formulated into virosomes. Adjuvants are formulated with liposomes. Both are concentrated and printed onto microarrays yielding a room-temperature stable sugar glass.

We demonstrate a three pronged technology using: (1) 0.3 μg of the antigen rHA from the 2019–2020 seasonal influenza strain B/Colorado/06/2017 produced in 293 cells, (2) 0.5 μg of the adjuvant QS-21 and 0.2 μg of the adjuvant 3D-(6-acyl) PHAD in a liposomal formulation and (3) a novel microarray of 37 microneedles each containing 10nL of vaccine material. Vaccinating Sprague Dawley rats with this configuration yielded ELISA IgG titers 100 times higher and HAI titers 10X higher than FluBlok as delivered IM, while using only 1/15 the dose of antigen.

2. Materials and methods

2.1. Production of recombinant antigen

Plasmid DNA encoding the full-length hemagglutinin of B/Colorado/06/2017 with a C-terminal thrombin cleavable 6X His tag under a modified CMV promoter was synthesized and prepared by ATUM Bio (Newark, CA). Expi293F cells (ThermoFisher, A14527) were grown in Expi293 Expression media (ThermoFisher, A1435101). Plasmid DNA was used to transfect these cells using ExpiFectamine 293 Transfection Kits (ThermoFisher, A14524). A second plasmid in the same vector, encoding the full-length neuraminidase enzyme from B/Colorado/06/2017, was co-transfected at equal dose to prevent clumping of cells during expression. Transient expression runs were performed in sterile, disposable 250 mL shaker flasks (ThermoFisher, PVB250) orbiting at 125 RPM in a humidified incubator at 8% CO_2. A temperature shift to 32 °C was performed at 24 h, cells were harvested 3 days after transfection and cell pellets stored at −80 °C. Cell pellets were washed with 1X PBS and solubilized with LDAO (N,N-Dimethyldodecylamine N-oxide; Sigma Life Science 40236) extraction buffer (2% LDAO, 20 mM NaP, 150 mM NaCl, 2 mM $MgCl_2$, pH 7.4) with periodic bath sonication. The lysate was digested with 100U of Benzonase (EMD Millipore 70746-10KUN) followed by two rounds of centrifugation for 20 min at 4,000 × g and 20,000 × g at 4°C. The cleared lysate was passed through a 0.2 μm filter and applied to a 1-mL HisTrap FF crude column (GE Healthcare, 11–0004-58) pre-equilibrated with LDAO IMAC Binding Buffer (0.5% LDAO, 20 mM NaP, 150 mM NaCl, 20 mM imidazole, pH 7.4), fitted to an AKTA FPLC (GE Life Sciences). Following a wash of 20 column volumes, LDAO-micelles of rHA were exchanged for octyl glucoside (Anatrace, O311) on-column by application of a 10 min linear gradient into OG Binding Buffer (1% octyl glucoside, 20 mM NaP, 150 mM NaCl, 20 mM imidazole, pH 7.4). After additional washing, rHA was eluted with a stepped gradient to 500 mM imidazole. The eluted micellized protein was concentrated on Amicon Ultra-15 30 K spin diafiltration columns (EMD Millipore, UFC903024), then dialyzed into VDB-OG (1% octyl glucoside, 10 mM NaP, 140 mM NaCl, pH 7.2) at 4 °C.

2.2. SDS-PAGE and Western blotting

Purified rHA and commercial FluBlok Quadrivalent vaccine (2019–2020 Northern hemisphere formulation, Protein Sciences / Sanofi) were evaluated for total protein content by BCA assay (ThermoFisher, #23227), before dilution into 1x Laemmeli buffer (Bio-Rad, #1610747) with 100 mM DTT (Bio-Rad, #1610610). Samples were heated at 90 °C for 10 min, then loaded onto a pre-cast 4–20% TGX polyacrylamide gel (Bio-Rad, #4561096). Separation was performed at 150 V for 45 min in Tris-Glycine buffer with 0.1% SDS (Bio-Rad, #1610732). The resulting gel was stained with SimplyBlue Safe Protein stain (Invitrogen, LC6060) and destained with deionized water to compare purity and size of material.

For Western blots, transfected cell material was solubilized in RIPA buffer (Cell Signalling, 9806S) and clarified by centrifugation after a freeze–thaw cycle. Recombinant HA digestion was performed by diluting 400 ng of rHA in 30 μL of 1x PBS containing TPCK-treated Trypsin (Sigma Life Sciences, T1426) at 2.5 μg/mL. Digestions were performed at 37 °C for 15, 30, 60, or 120 min before addition of Laemeli buffer to 1x and DTT to 100 mM. Reactions were then heated to 90 °C for 10 min, prior to loading at 150 ng rHA per well. After electrophoresis, TGX Gradient gels (4–20%) were transferred onto nitrocellulose membranes (Bio-Rad #1620213) in 1x Tris-Glycine buffer (Bio-Rad, #1610734) with 10% methanol for 60 min at 100 V. Membranes were blocked for

1 h in 5% (w/v) nonfat milk (Bio-Rad #170–6404) in 1x TBS buffer (Bio-Rad, #1706435), then incubated with monoclonal antibodies for 2 h. For detection of the 6xHis tag on the C-terminus of our rHA antigen, a rabbit monoclonal antibody was used (Cell Signaling, D3I10 XP) at 1:5000 in TBST with 0.5% (w/v) non-fat milk.

To detect influenza B HA, Mouse Monoclonal Antibody to Recombinant HA1 Domain from Influenza B/Brisbane/60/2008 (Victoria Lineage), Clone ATCC 008 1D11, FR-1333, was obtained through the International Reagent Resource, Influenza Division, WHO Collaborating Center for Surveillance, Epidemiology and Control of Influenza, Centers for Disease Control and Prevention, Atlanta, GA, USA. Three 5-minute washes with TBST (1xTBS with 0.05% v/v Tween® 20 – Fisher Scientific, BP337-100) were then performed. Mouse monoclonal antibody was detected with donkey anti-mouse-HRP antibody (Jackson labs, 715-035-150) at 1:2500, while rabbit monoclonal antibody was detected with goat anti-rabbit HRP antibody (Bio-Rad #172-1019). In both cases, secondary antibody dilutions were performed in TBST + 0.5%(w/v) nonfat milk, and incubated for 1 h, followed by three additional 5-minute 1x TBST washes and one wash in 1x TBS. Blots were then visualized with Pierce 1-step Ultra TMB blotting solution (Thermo Scientific #37574) for 5–20 min.

2.3. Production of virosomes

Virosomes were prepared by incubating octyl-glucoside-micellized rHA at 0.2 mg/mL with a lipid mixture at 1 mg/mL, consisting of 67% (w/v) DOPC (1,2-dioleoyl-*sn*-glycero-3-phosphocholine) and 33% (w/v) plant cholesterol (Avanti Polar Lipids, 850,375 and 700100) for 30 min at 4 °C prior to loading into a 10 K dialysis cassette (Thermo Scientific, #66380) and dialyzed against a solution of 1x VDB (140 mM NaCl, 10 mM NaP, pH 7.2) to remove the detergent. After multiple buffer changes, virosomes form spontaneously. Virosomes were buffer exchanged by diafiltration to 1x VDB-tre (15% (w/v) α, α-trehalose dihydrate (Pfanstiehl, T104-4), 10 mM NaP, 140 mM NaCl; pH 7.2) and final concentration was performed on Amicon Ultra-0.5 30 K spin columns (EMD Millipore, UFC503096) at 4000*g* and 4 °C.

2.4. Liposome adjuvant formulation

Empty DOPC/cholesterol liposomes were prepared in an identical manner as the virosomes above but without the addition of the rHA. 3D-(6-acyl)-PHAD (Avanti Polar Lipids, 699855) was then loaded into liposomes by addition of 10 μL of 10 mg/mL 3D-(6-acyl)-PHAD dissolved in DMSO to 490 μL of liposomes. This mixture was incubated for 45 min at room temperature and buffer exchanged into 1x VDB-tre by diafiltration. During the final buffer change, the 3D-(6-acyl)-PHAD loaded liposomes were supplemented with 100 μg QS-21 (Croda Health Care) resuspended in 1x VDB-tre, then sufficiently concentrated to enable printing of arrays at a final dose of 200 ng of 3D-(6-acyl)-PHAD and 500 ng of QS-21 per VaxiPatch array.

2.5. Microarray design and Fabrication

Computer Aided Designs (CAD designs) were produced to Verndari specifications under a Services Agreement by the UC Davis College of Engineering and the Biomedical Engineering BME TEAM Design, Prototyping and Fabrication Facility. CAD drawings were sent to Tecomet, Inc. (Azusa, CA) where the CAD drawings were translated into production files. Microarrays were fabricated by photochemical etching of 3 mil-thick (75 μm) medical grade stainless steel (SS304) foil. Designs for Verndari microarrays were improved in an iterative fashion, with testing of various numbers and configurations of microneedles per array. The microneedle tips themselves were also developed over several versions; altering well dimensions, needle length, and edge characteristics. These refinements resulted in the R11 design described in this work, which bears 37 microneedles per array, in a 1.2 cm round format. Imaging of microarrays, individual microneedles, as well as quantitative distance measurements and surface roughness (Sa), were performed with a Leica DVM-6 Digital Microscope.

2.6. Microarray loading and packaging

Microarrays were designed specifically to utilize BioDot, (Irvine, CA) microfluidic dispensing devices for API loading. These dispensing devices can be customized for mass production and are commonly used in the production of FDA-approved Lateral Flow Immunodiagnostics. Microfluidic dispensing is done in two dimensions (X, Y-plane). Sheets of R11 microarrays as described above were loaded with vaccine using a BioDot AD1520 microfluidic dispenser. These instruments can be custom programmed to load vaccine material to entire sheets of arrays in series from a single print head, or in parallel if multiple injector valves are utilized. For research purposes the instrument rapidly fills the etched wells of all 37 individual microneedles in the two-dimensional X, Y-plane with a single 10 nL drop for each tip. This dispensing cycle takes about 9 s per array. The liquid drops undergo initial drying in the first 10 – 15 s after dispensing. Once the microarrays were loaded and dried, the microneedle tips were tilted into the Z-plane. Vaccine loaded, Z-plane-oriented microarrays were placed in heat sealable foil pouches (AMPAC, No. KSP-150-1 MB, 4.5 mil) with a three gram bagged desiccant pack (W.A. Hammond Drierite Co., LTD, No. 60013 or 60013T) and sealed with an Accu-Seal heat sealer (model 8000-GV, San Marcos, CA). Bagged VaxiPatches were stored overnight at 20 °C to complete drying.

2.7. Imaging and delivery assessment for printed arrays

Imaging of printed vaccines was performed with a Leica DVM-6 Digital Microscope. In order to better visualize sugar glasses and assess delivery, print mixes were formulated with 0.5% (w/v) FD&C Blue No.1 (Spectrum Chemicals, FD110, Gardena CA, USA) prior to deposition on microarray tips. FD&C blue dye No. 1 was FDA approved for use in food in 1969 and in drugs and cosmetics in 1982. Qualitative assessment of delivery involved digital microscopy of post-treatment arrays recovered after animal treatments, as compared to non-applied control arrays. Photos of the application sites on the skin of rats were also examined for dye deposition. For quantitative assessment, dye from experimental microarrays was eluted in 150 μL of PBS, alongside a set of control microarrays containing full print doses. 100 μL of this eluent was analyzed by absorbance (620 nm, accuSkanFC microplate reader type 357, Thermo Fisher Scientific) along with a standard curve of FD&C No. 1. The percentage delivered was evaluated by comparing residual dye on experimental microarrays remaining after animal treatment against elutions of non-applied control microarrays still containing the full dose.

2.8. Animal studies

All animal studies were approved by the UC Davis Institutional Animal Care and Use Committee (IACUC) Protocol No. 21302 and were performed by the UC Davis Mouse Biology Program (MBP). Male and Female Sprague Dawley™ rats were purchased from Envigo (Livermore, CA) at 8–10 weeks of age. Animals were group housed (3 per cage) in Thoren caging systems. One to two days before treatment, patches of hair were removed from the rear dorsal area of the rats by shaving, followed by treatment with depilatory cream. For array applications, animals were anesthetized by

inhalation with 5% isoflurane, and maintained at 2.5–3% via use of a nose cone. Application sites were scored on a modified Draize scale for erythema and oedema prior to and 1 h post-VaxiPatch treatment, with follow-up evaluations on the following day. VaxiPatch arrays were applied to rats manually by maintenance of light finger pressure for 5 min, then removed and re-packaged for later analysis of residual dye. Serum samples were collected from immunized animals at prior to vaccination and at weekly intervals for four weeks, n = 6 for each group (3 of each gender). Intradermal and intramuscular injections were performed at the right hind limb (thigh) with 50 μL of vaccine material, diluted to target dose with sterile phosphate-buffered saline solution.

2.9. ELISA assay

Assay plates (Corning 3601) were coated overnight at 4 °C with rHA at 0.5 μg/mL in 100 mM Carbonate buffer (Alfa Aesar, J62610). The vaccine antigen (purified, full-length rHA from B/Colorado/06/2017) was used as the coating antigen. The plates were washed 3x with Tris-buffered saline (TBS, Bio-Rad 170-6435) with 0.05% Tween-20 (Fisher, BP337-100) – TBST, and blocked with 5% (w/v) non-fat dry milk (Bio-Rad, 170-6404) in TBS for 2–3 h at room temperature. After one additional TBST wash, rat sera (generally 1:100–1:312,500) and positive control monoclonal antibody (Immune Tech, IT-003-B21M4, at 1:6,000–1:750,000) in 1% milk/TBST were loaded in duplicate and incubated for 2 h at room temperature, followed by 4 washes with TBST. Goat anti-rat-IgG HRP antibody (Jackson Labs, 112-035-143), at 1:10,000 in 1% (w/v) non-fat milk/TBST, was added and incubated for 1 h at room temperature for experimental and blank wells. For monoclonal antibody control wells, donkey anti-mouse-IgG HRP antibody (Jackson labs, 715-035-150) was added at 1:5000 in 1% milk/TBST. After four additional washes, 100 μL of substrate was added (R&D systems, DY999), and incubated at room temperature for 30 min. The reaction was stopped by addition of 50 μL 2 N sulfuric acid (R&D systems, DY994). Absorbance was read at 450 nm. Positivity was defined as absorbance beyond twice the average blank well of the plate. Readings were taken with an accuSkanFC microplate reader type 357 (Thermo Fisher Scientific).

2.10. Hemagglutination and hemagglutination inhibition assays

Fresh turkey erythrocytes (Innovative Research, ITKRBC5P30ML, Novi MI) were washed 5x with cold PBS and calibrated to a 0.5% packed cell volume suspension (PCV, approx. 40 M cells/mL). Recombinant HA or controls were serially diluted in PBS in V-bottom assay plates (Costar 3363) before addition of 50 μL of the turkey RBC suspension. Plates were incubated at room temperature for 30 min to allow settling of RBCs. A tipping step was employed to induce running in non-agglutinated wells prior to documentation.

For hemagglutination inhibition assays, washed single-donor O + human erythrocytes (Innovative Research, IWB3ALS40ML, Novi MI) were sourced and washed as above, with final calibrated suspensions at of 0.75% PCV (~60 M/mL). BPL-inactivated B/Colorado/06/2017 virus was titered for HA activity against these suspensions in U-bottom assay plates (Falcon 353910, Corning Inc). 2018–2019 WHO Antigen, Influenza B Control Antigen, Victoria Lineage (B/Colorado/06/2017), BPL-Inactivated, FR-1607, was obtained through the International Reagent Resource, Influenza Division, WHO Collaborating Center for Surveillance, Epidemiology and Control of Influenza, Centers for Disease Control and Prevention, Atlanta, GA, USA. This BPL standard was used to prepare a stock at 8 hemagglutinating units (HAU) per 50 μL in 1x PBS, which was confirmed by back titration.

Sera from experimental Sprague-Dawley rats was pre-treated with kaolin as described in the USDA CVB Testing protocol (SAM 124.05). In brief, serum was diluted 5-fold in a 10% kaolin solution (Acros Organics, 211740010) in 1x PBS. This suspension was periodically vortex mixed for 20 min, then pelleted by centrifugation at 800*g* for 20 min. One-half volume of concentrated, washed human erythrocytes was then added along with 3.5 volumes of additional PBS. Suspensions were gently mixed periodically for 20 min, then centrifuged at 400*g* for 20 min to remove RBCs. The cleared supernatant was then collected and used for inhibition testing.

Two-fold serial dilutions of kaolin-treated sera were prepared in U-bottom plates in 25 μL volumes, to which 25 μL of BPL antigen was added (4 HAU / well). As a positive control, hyperimmune sheep antisera against HA of a related strain (B/Brisbane/60/2008) was tested in parallel (16/192, NIBSC, Potters Bar, UK). Wells were mixed by gentle tapping of the plate, and allowed to incubate at room temperature for 45 min. Next, 50 μL of the 0.75% RBC suspension was added per well. After mixing and another 60 min at room temperature, plates were examined for evidence of inhibition, as evidenced by formation of rings of settled cells.

2.11. Vaccine material potency and stability studies

Vaccine potency was determined by a standard procedure of single radial immunodiffusion (SRID). Antigens and antisera specific to B/Colorado/06/2017 (CO'17) were obtained from the National Institute for Biological Standards and Control (18/104 and 18/170, NIBSC, Potters Bar, UK). Samples were treated with 1% Zwittergent 3–14 detergent (EMD Millipore) for 30 min at room temperature, then loaded to antiserum-containing 1% agarose gels and allowed to diffuse outwards for 24 h in a humidified chamber. Gels were then dried and adhered to GelBond substrate (GE Life Sciences), followed by staining with GelCode Blue Safe Protein Stain (Thermo Scientific). After de-staining in water, the gels were imaged, and images were analyzed with the ImageJ software package (NIH) to calculate annulus precipitation zones of each loaded sample. From the data, a standard curve for the HA protein was generated and strain-specific SRID potency values were determined.

For stability studies, concentrated formulated virosomes were prepared as they would be for VaxiPatch array printing (15% trehalose, 0.5% FD&C blue dye). This material was then deposited as 1 μL aliquots in open 0.5 mL microcentrifuge tubes, which were stored in sealed foil bags containing desiccant packs at 20 °C overnight to achieve initial drying. These bags were then segregated and stored at temperatures of 20, 40, or 60 °C. At designated time points, samples were unsealed, reconstituted in PBS, and subjected to SRID assay to determine the extent of remaining HA potency.

2.12. Statistical analysis

ELISA IgG titers and HAI titers at week 4 post-vaccination were subjected to a one-way ANOVA test followed by post-hoc Tukey's HSD tests to establish statistical significance. These calculations were performed with Microsoft Excel.

3. Results

3.1. Fabrication of stainless steel microarrays.

Microarrays were fabricated by three-dimensional photochemical etching of medical grade stainless steel 3 mil (75 μm) foil by a proprietary process (Tecomet, Azusa, CA). Three-dimensional photochemical etching of stainless steel foil has not been previously described. Through an iterative process starting with revision 1, we, together with Tecomet, made incremental improvements

reaching revision 11. The average microneedle length (n = 39) with bevel is 703.2 μm with a standard deviation (SD) of 5.2 μm, microneedle width with bevel is 306 μm (SD 6.3 μm), well length is 406.6 μm (SD 4.2 μm); well width is 213.1 μm (SD 2.8 μm), well depth is 43.9 μm (SD 8.2 μm); hinge depth is 30.0 μm (SD 3.9 μm). The average microneedle length when tilted 90° into the Z-plane is 596.95 μm (SD 8.5 μm, data not shown). The surface roughness (Sa) as determined with the Leica digital microscope software algorithm for a region of interest (ROI) in the bottom of the half-etch well is 0.14 μm (SD 0.084 μm). In comparison, a measurement of Sa for a ROI on the bright bevel of a Becton Dickenson 32G needle is 1.5 μm (SD 1.13 μm), whereas the Sa of a ROI on the dark bevel on the tip of the Becton Dickenson needle is 4.35 μm (SD 1.13 μm). Thus, the smoothness of the Verndari microarrays compares favorably to other stainless steel medical devices in current use.

3.2. Purified recombinant HA antigen from mammalian cells is active in functional assays and recognized by B-Victoria specific antibody

The full-length HA protein from influenza strain B/Colorado/06/2017 was produced by transient transfection of a synthetic expression construct into a scalable high-density mammalian expression system (Expi293F, ThermoFisher). Cell pellets from these cultures were treated with detergent to extract rHA into micelles, and extracts were purified to homogeneity on the basis of a C-terminal 6xHis tag. Fig. 1A shows increasing concentrations of the purified material on a 4–20% gradient SDS-PAGE gel, as compared to a comparable quantity of the recombinant vaccine product FluBlok. Note the more heterogeneous and slightly smaller apparent mass of insect-cell expressed quadrivalent FluBlok product, which consists of four different rHA proteins. We expect this material to have less complex glycosylation than our mammalian cell-expressed rHA0. Our recombinant HA was recognized robustly by several monoclonal antibodies specific for Victoria-lineage Influenza B HA; one of which is demonstrated in Fig. 1B. Extracts from transfected ExpiCHO and Expi293 cells were examined by Western blotting, displaying highly specific signals at the anticipated size of ~ 80 kD. The rightmost experimental lane in Fig. 1B was loaded with Expi293 lysate transfected with an alternative construct using a heterologous N-terminal signal sequence.

Identity and structural integrity of the purified rHA0 was also tested by digestion with TPCK-treated trypsin at 2.5 μg/mL, as shown in Fig. 1C. Incubation for 15 min or more with trypsin led to accumulation of a smaller His-tagged product at ~ 32 kD, consistent with proper HA2 cleavage. Finally, purified rHA0 was shown to efficiently agglutinate turkey erythrocytes in an HA assay; with complete agglutination down to 1.95 ng per well (Fig. 1D).

3.3. Incorporation of purified recombinant HA antigen into virosomes

To enhance immunogenicity of our recombinant antigen, purified full-length rHA was incorporated into virosomes by dialysis. Size and uniformity of the resulting nanoparticles were measured by dynamic light scattering (DLS) on a Malvern Zetasizer Nano-ZS (Malvern Instruments). Two measurements were taken for each of three independent virosomal preparations. The Z-average size of these preparations was 165.27 +/- 12.69 nm in diameter with a PdI

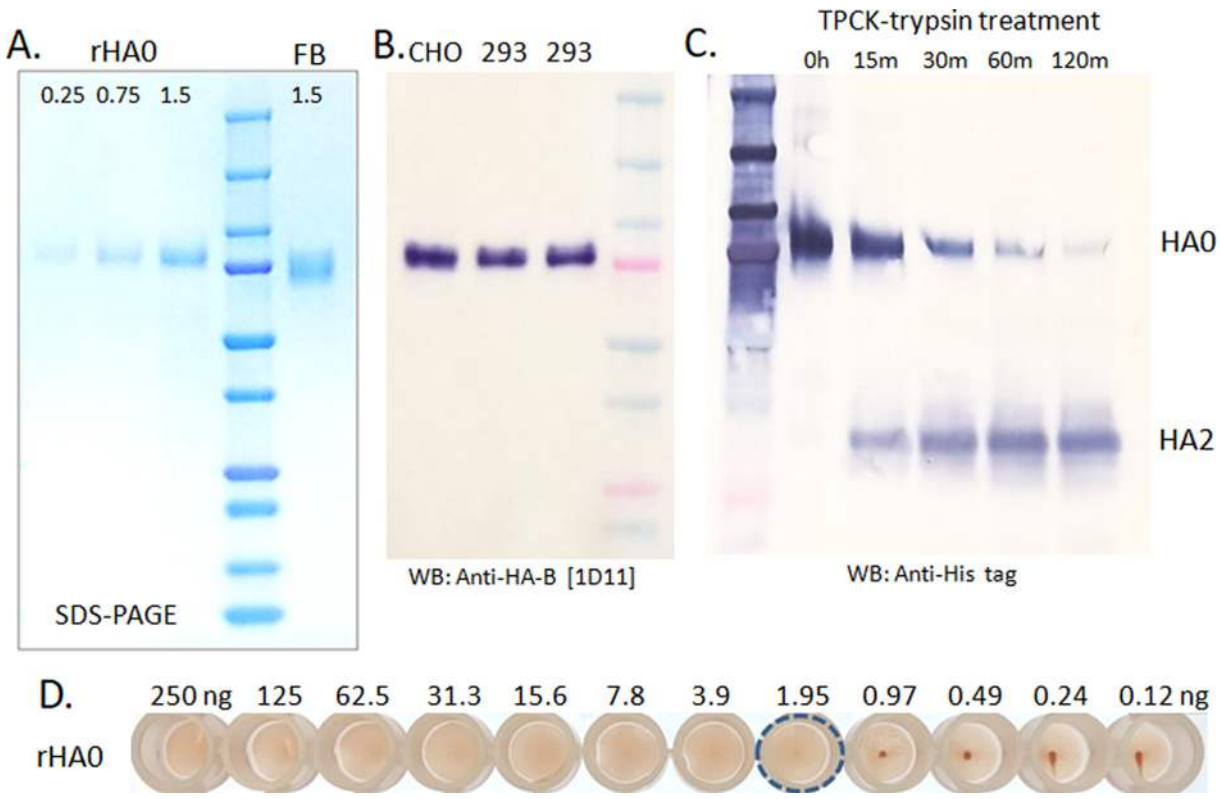

Fig. 1. Characterization of rHA. a) Purified rHA is shown on an SDS-PAGE gel, loaded at 250, 750, and 1500 ng per lane. The far right lane was loaded with 1500 ng of commercial FluBlok vaccine as a comparison. b) Lysates from ExpiCHO (left lane) or Expi293 (center lanes) transfected with rHA constructs are shown after detection with a monoclonal antibody specific to Victoria-lineage influenza B HA. The third lane was transfected with a vector that included a heterologous signal sequence, while the leftmost two lanes received DNA coding for the native sequence. c) Purified rHA was digested with TPCK-trypsin at 2.5 μg/mL for increasing durations as shown in the label. After digestion, this material was analyzed by Western blotting with a rabbit monoclonal specific to the C-terminal 6xHis tag. Thus the tag visualizes both uncleaved rHA (HA0) and the C-terminal HA2 fragment. d) A 30-minute hemagglutination assay was performed with serial dilutions of rHA from 250 ng/well, on fresh turkey RBCs. The dotted circle indicates complete agglutination at 1.95 ng/well.

of 0.15 +/- 0.03. Representative traces of the size distribution by intensity for each of the three preparations are displayed in Fig. 2A and a summary table of all of the measurements is displayed in Fig. 2B. Incorporation of rHA0 into virosomes mediated an increase in hemagglutination activity when compared to rHA0 alone, with complete agglutination occurring at a substantially lowered rHA dose of 0.5 ng per well (Fig. 2C).

3.4. Loading and preparation of VaxiPatches

Two empty R11 VaxiPatches are shown in Fig. 3A, while still attached to a full stainless steel sheet of arrays. Note the 37 tips aligned flat in the X/Y plane, as well as the side notches for alignment. When assembled with medical tape, snap disk applicator, and plastic liners, a prototype VaxiPatch product formatted for human use is shown in Fig. 3B. For immunogenicity testing, concentrated virosomes were formulated with or without adjuvant at a final concentration of 15% (w/v) trehalose (Pfanstiehl Inc, Waukegan IL, USA) and 0.5% FD&C Blue No. 1 dye (Spectrum Chemical FD110, Gardena CA, USA). Virosomes for animal treatments were generally formulated at 0.8108 mg/mL to achieve a 300 ng dose per patch (0.37 μL total dispensed volume). Adjuvanted patches were formulated with QS-21 at 0.5 μg per dose, and the TLR4 agonist 3D-(6-acyl)-PHAD at 200 ng per dose. Dispensing of formulated vaccine material was performed with a BioDot AD1520C microfluidic printer in batch mode at 10 nL per tip. After initial drying, the array tips were aligned into the Z-axis using a bending jig. A high-resolution side image of a loaded array is shown in Fig. 3C. Z-aligned arrays were then affixed to squares of waterproof medical tape to aid in direct-pressure applications, then sealed into foil bags with 3-gram desiccant packs overnight at 20°C to complete the drying process.

3.5. Immunogenicity of VaxiPatch-delivered recombinant influenza vaccine

In the context of this study, a total of 24 Sprague-Dawley rats were treated with rHA virosome-loaded VaxiPatch arrays, all as a single-dose regimen. Equal numbers of male and female rats were treated (3 of each gender per group). Applications were performed manually by application of light direct pressure for 5 min, as the human-format snap device applicator assemblies shown in Fig. 3B proved to be too large for reliable use with rodent models. The posterior dorsal area was used for all treatments to provide reasonable support for array application.

Assessments of the application sites for erythema and oedema on 5-point modified Draize score were performed for all VaxiPatch applications. Even for dual-adjuvanted VaxiPatch treatments, no redness or swelling was noted associated with application of the arrays. Based on elution assays of post-application patches, the release of treatment ranged from 80 to 96.2% for these groups, with an average of 87.7% and a standard deviation of 4.55%.

As a comparator, the quadrivalent insect-cell derived recombinant influenza vaccine FluBlok was injected intramuscularly at 1/10th a human dose (4.5 μg per strain) for six animals. As an additional control, six animals were also injected intramuscularly with rHA virosomes at the same dose as FluBlok. Pre-immune and weekly bleeds were performed on all animals, with the exception of the female IM injection animals, which were only sampled on days 0 and 28 due to scheduling conflicts. Serum was banked for analysis of specific IgG titers by ELISA assay, against the cognate antigen.

As is shown in Fig. 4, robust specific IgG titers were detected by 14 days post-vaccination in both adjuvanted VaxiPatch groups, with some increases through day 28. When applied without adjuvants, virosome-loaded VaxiPatches were comparable to the 15-fold higher-doses of IM injected material. Three of the 30 animals in this study (10%) also exhibited weak (positive only at 1:100) baseline reactivity with the coating antigen in their pre-immune samples; not uncommon among outbred animals.

For the final day 28 post-vaccination samples, a dot plot of ELISA IgG titer is shown in Fig. 5 with statistical comparisons between the treatment groups. Based on this analysis, we see that incorporation of either adjuvant formulation is associated with a highly significant ($p < 0.01$) increase in IgG titers over non-adjuvanted VaxiPatches or IM injected FluBlok. Further modest

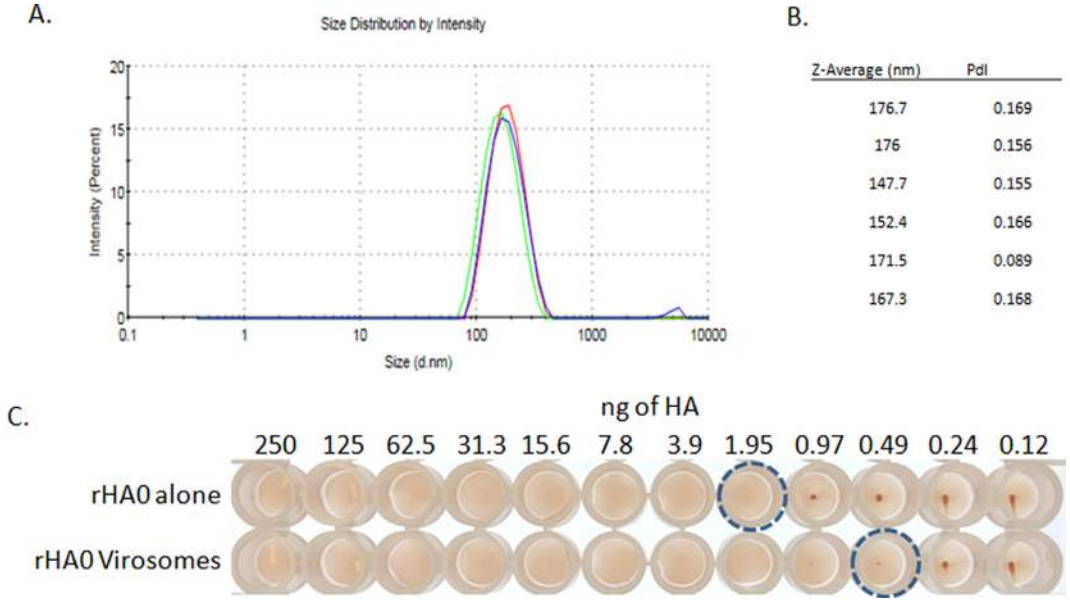

Fig. 2. Characterization of Virosomes. a) Dynamic light scattering was performed on three independent batches of rHA virosomes, which are overlaid on the size distribution plot as shown. b) Measurements of Z-average diameter and polydispersity index PdI are shown for two measurements each on the three batches. c) Hemagglutination of turkey RBCs was enhanced in the context of equal loading for rHA content, suggesting higher-order structure for the rHA in virosomal nanoparticles. Dotted circles indicate complete agglutination.

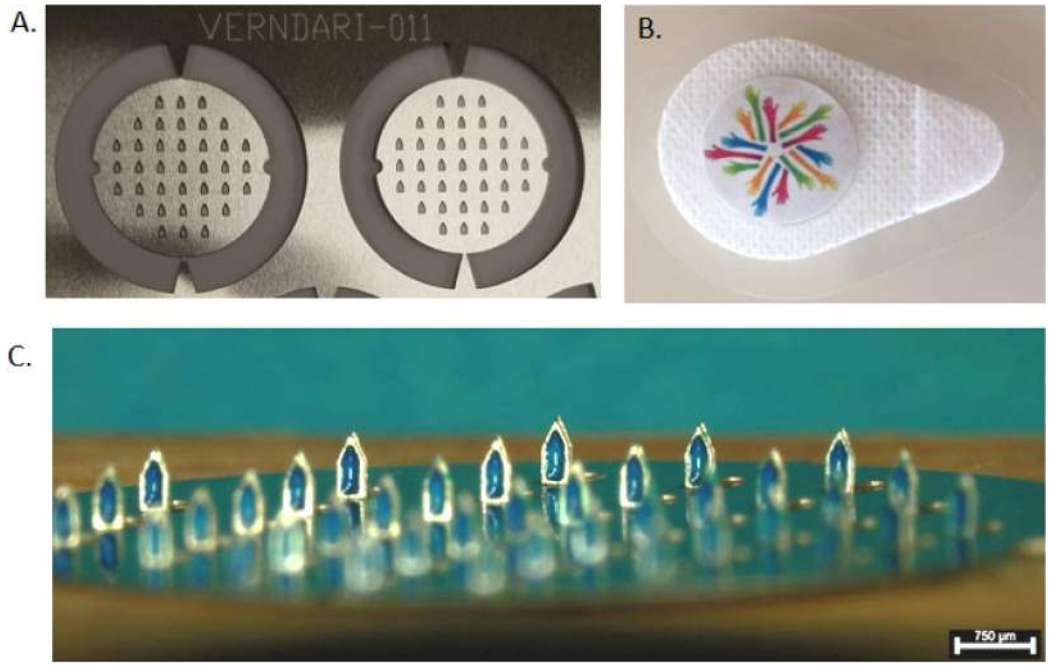

Fig. 3. Printed VaxiPatch arrays. a) Two R11 VaxiPatch arrays are shown in the context of an etched sheet of stainless steel, prior to singulation, printing, and re-orientation of tips. b) A completed human-format VaxiPatch with adhesive tape, snap applicator, and plastic protective liner is shown. Light pressure on the center of the logo triggers actuation of the snap device. c) A narrow-focus, high resolution image of a loaded, Z-plane oriented VaxiPatch array.

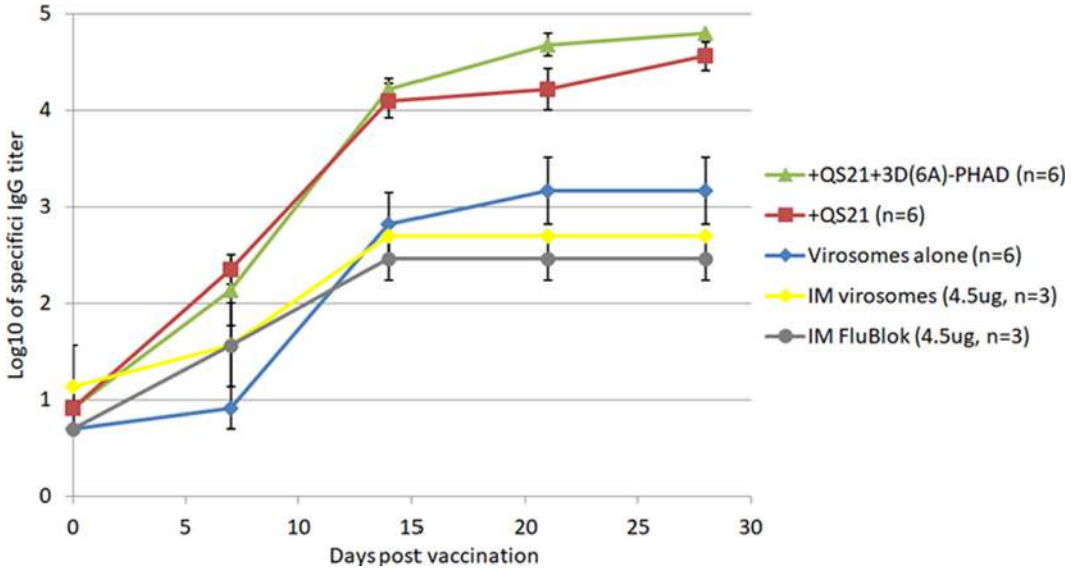

Fig. 4. Time course of IgG ELISA responses. Averages of log-transformed endpoint IgG titers against the recombinant B/Colorado/06/2017 antigen are shown here for each sampled time point, with error bars representing standard error of the mean. All three VaxiPatch-delivered groups have N = 6, with equal numbers of each gender. For female IM injection control animals, day 7–21 samples were not available, so only the males from these two groups are plotted (N = 3). Serum samples which were negative at the lowest dilution tested (1:100) were assigned an arbitrary titer of 5. VaxiPatch antigen doses were 0.3 μg per animal, while IM injections used 4.5 μg per dose.

improvements in GMT titers were observed with incorporation of 3D-(6A)-PHAD, but these fell below the threshold of statistical significance.

3.6. Functional analysis of VaxiPatch-driven immune responses

While specific IgG titer analysis by ELISA provides important demonstration of the magnitude of an immune response, it does not provide any indication of vaccine efficacy. A key advantage of influenza as a model system is the existence of well-established surrogate markers for efficacy based on the neutralization of HA activity. For the purposes of clinical trials in humans, inhibition of the agglutination of RBCs by serum at 1:40 or higher dilution is a rough correlate of protection against the cognate strain used in the hemagglutination inhibition assay (HAI). Adaption of this assay for Sprague-Dawley rat serum was complicated by high levels of non-specific inhibition in naïve rat serum, which increase after heat inactivation. Pre-treatment of rat serum with kaolin, followed by pre-absorption with RBCs, eventually proved to be highly effective at removing this non-specific inhibition while retaining

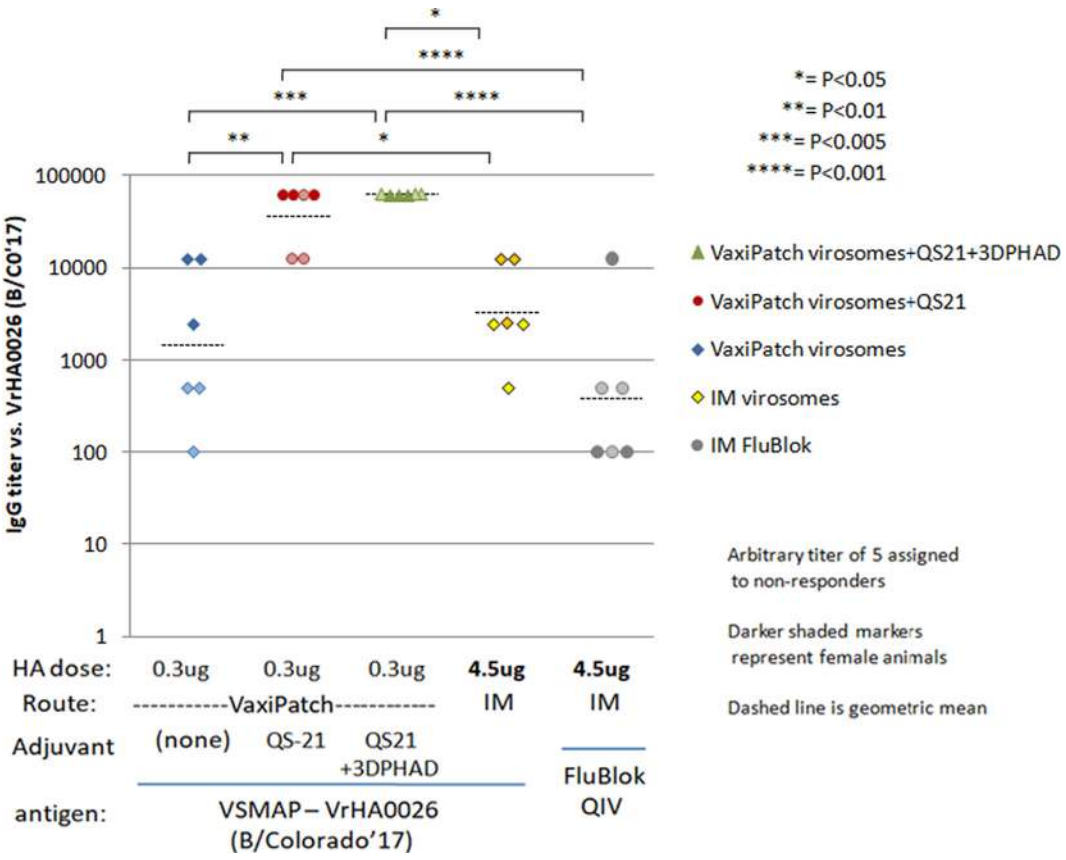

Fig. 5. Week 4 IgG ELISA titers. To provide more granular information on variation within these groups, a dot plot is shown for the day 28 serum samples. Dashed lines indicate geometric mean titers among groups. Darker shading indicates female animals within each group. Statistical significance as determined by post-hoc Tukey's HSD tests are shown above the plot, with indications of the p-values classification for each.

high levels of strain-specific activity in vaccinated rats with elevated IgG titers.

Week 4 sera from all 30 vaccinated animals were analyzed by HAI, using a WHO standard BPL-inactivated virion standard (B/Colorado/06/2017) as the target agglutinating antigen. Levels of inhibition for each animal are shown in Fig. 6, along with statistical comparisons between groups. Eleven of twelve animals vaccinated with adjuvanted VaxiPatches achieved HAI titers of 1:40 or above, with eight of those scoring 1:80 or higher from the single intradermal vaccination. Inhibition titers from the IM injection controls were very weak, with only two of twelve animals achieving a 1:40 titer (both were from the virosome injection group). The non-adjuvanted VaxiPatch group had higher GMT HAI titers than IM injection controls, but not enough to be statistically significant, as there was significant animal to animal variation. Co-formulation of either adjuvant preparation yielded highly significant improvements over IM injection groups despite 15-fold lower antigen doses. As with the IgG ELISA data, the animals receiving 3D-(6A)-PHAD adjuvant in addition to QS-21 had a slightly higher GMT HAI titer, but the difference fell below the threshold for significance.

3.7. Stability of virosomes

Drying of vaccine antigens in a sugar glass state can allow for impressive levels of thermostability. We employed the industry-standard assay for HA-based vaccine potency, the single radial immunodiffusion assay (SRID) to investigate the potential of our virosomal rHA to retain activity without refrigeration. As our printed VaxiPatch doses are so low compared to standard influenza vaccines (50-fold lower than traditional egg-based vaccine, 150-fold lower than FluBlok IM), it is technically challenging to perform accelerated aging studies on the printed arrays (20 or more arrays must be eluted and pooled to achieve a dose within the limited linear range of the SRID assay (~8–50 μg/mL). As an alternative, we prepared print mixes with a 2-fold increased HA content (1.68 mg/mL rHA) and used these to set up 1-μL drops for desiccation and storage. After initial drying overnight at 20°C, these samples were segregated to 20, 40, and 60°C temperatures for 8 weeks of storage. At the end of this time, reconstituted virosomes retained 64.07%, 65.43% and 56.33% of their potent HA when stored at 20, 40, and 60 °C, respectively (Fig. 7) as measured by B/Colorado/06/2017-specific SRID.

4. Discussion

This study demonstrates the potential of combining a mammalian cell-expressed recombinant antigen with an effective adjuvant system and an intradermal delivery platform. We have focused on development of a monovalent antigen based on the 2019–2020 Victoria-lineage influenza B strain, B/Colorado/06/2017. As we start from a synthetic protein sequence, we were able to match the original isolate of the recommended strain exactly. Traditional split-virion influenza vaccines are limited to strains that can be propagated efficiently in eggs. It was unexpected to observe such poor responses to the commercial FluBlok vaccine comparator, on the basis of previous experiments at Verndari with prior seasonal formulations of FluBlok. However, our previous studies focused primarily on the H1N1pdm09 strain A/Michigan/45/2015, and pre-dated the inclusion of

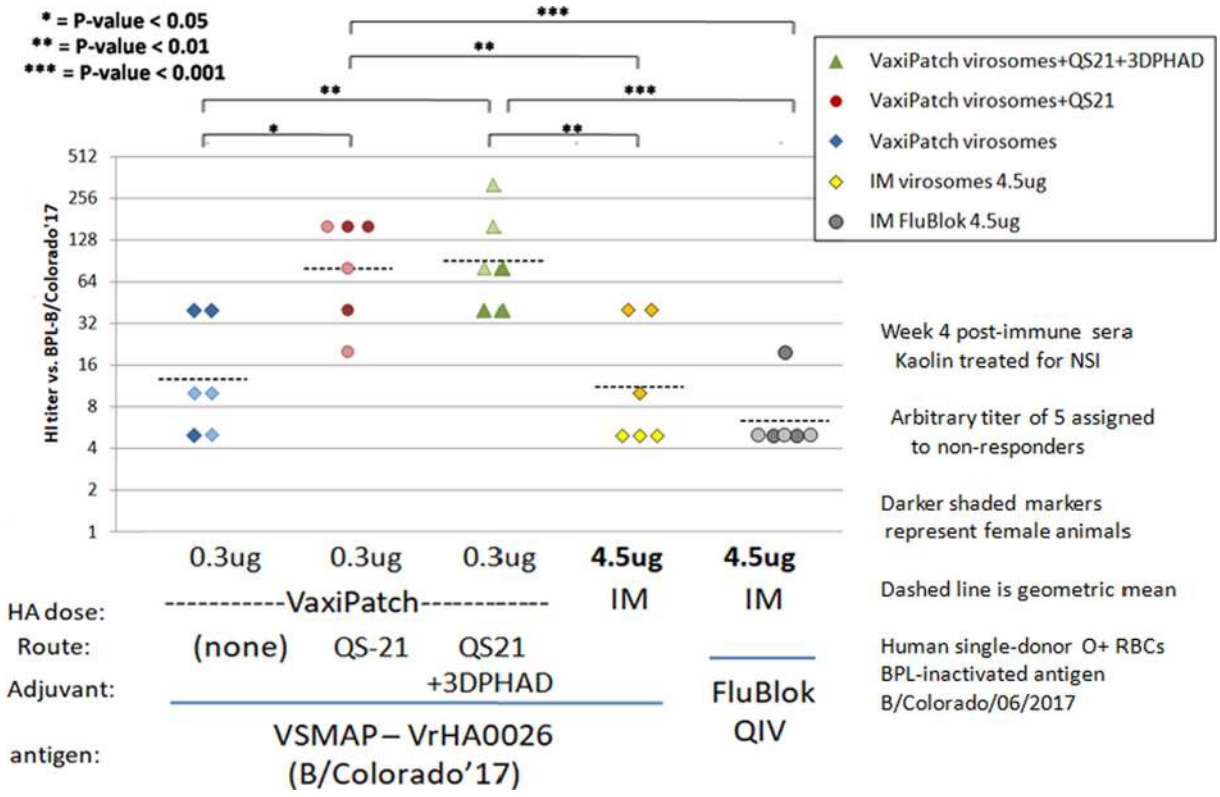

Fig. 6. Hemagglutination Inhibition Titers at Week 4. Vaccinated rat serum was tested for its ability to inhibit the agglutination activity of a cognate WHO reference antigen, BPL-inactivated B/Colorado/06/2017 virus on human RBCs. Inhibition titers ranged from 1:10 to 1:320 after a single vaccination. Samples which failed to inhibit agglutination at 1:10 were assigned an arbitrary titer of 5 for visualization and analysis. Dashed lines represent GMT titers within each group, and darker shades of color are used to indicate female animals among the groups. Statistical significance is indicated where present, based on post-hoc Tukey's HSD tests.

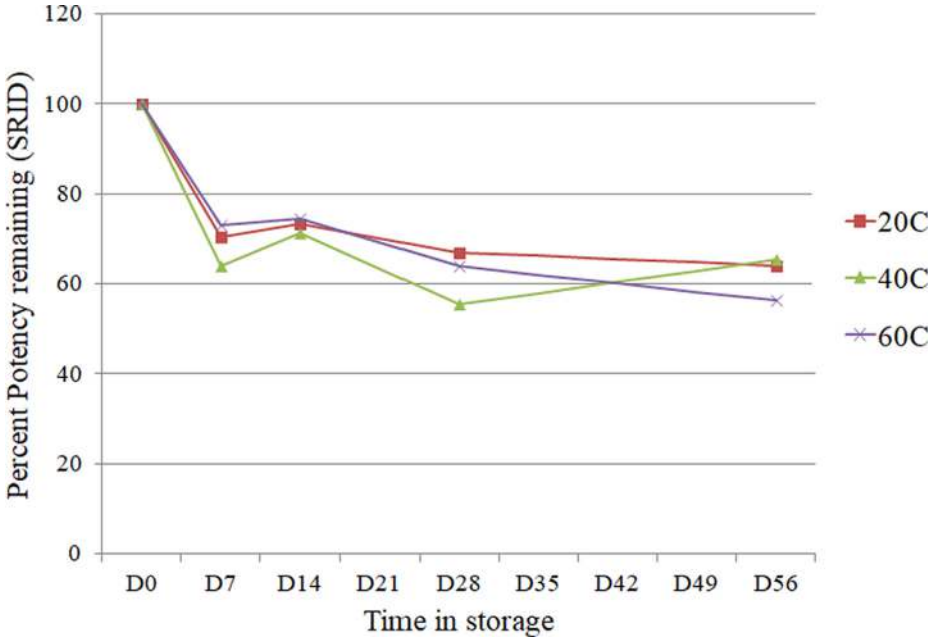

Fig. 7. Stability of Formulated Virosomes. Formulated print mix including rHA, trehalose, and dye, was aliquoted as small drops (1 μL each) and dried overnight under desiccation prior to segregation to elevated temperatures for extended storage. At the time points indicated (0–56 days), material was reconstituted in PBS and tested for retention of antigenic potency by strain-specific SRID assay. Average μg/mL potency at day 0 was used as a reference point for retention of percent potency in the accelerated aging groups.

B/Colorado/06/2017 to the list of recommended strains. Interestingly, the FluBlok product used in this study actually utilizes protein sequences from a closely related strain, B/Maryland/15/2016, in place of B/Colorado/06/2017. Outside of the N-terminal signal peptide, there is only one amino acid difference between the two proteins, but this may nonetheless have contributed to poorer

specific IgG titers against a B/Colorado rHA antigen, as well as diminished HAI titers against a BPL-inactivated B/Colorado/06/2017 antigen. While this remains a possibility, it should be noted that NIBSC supplies B/Maryland'16 antigen as the standard to use for B/Colorado/06/2017 SRID reagents, so a functional equivalence is strongly presumed.

While dose sparing was not directly tested in this study, the 15-fold reduced doses of rHA used in VaxiPatch presentations were comparable or more effective than IM injected material based on GMT titers. The most striking result demonstrated here is the clear advantage to using an adjuvant system incorporating the saponin adjuvant QS-21. While it remains unclear whether the TLR4 agonist 3D (6A)-PHAD has a strong effect, both QS-21 containing formulations had strong statistical significance over IM injected or non-adjuvanted comparators. Importantly, no redness or swelling were associated with use of QS-21 at the doses used in this system, which are 100-fold lower than those present in the AS01b-adjuvanted Shingrix vaccine, which has been widely associated with injection site pain and redness. The presence of cholesterol in the virosome and liposome components is sufficient to potently quench hemolytic activity of QS-21 even up to higher doses based on internal hemolysis assays (unpublished observations). The AS01b adjuvant system also includes a TLR4 agonist (MPL), similar to our 3D-(6A)-PHAD, but at an equal dose by mass (50 μg per dose). It is possible that further escalation of our TLR4 component dose might yield more synergistic effects. Alternatively, presence of a TLR agonist may help drive development of cell-mediated immunity, which would not be detected by the assays employed in this study.

The limited stability study described here is highly preliminary, but it provides important evidence that sugar glass stabilization is effective to protect a mammalian cell-derived recombinant antigen, even when it has been formulated into a lipid/cholesterol particle. Further studies will investigate the stability of co-formulated adjuvants and their effects, if any, on HA antigenic potency, as well as the potential role of contact surface material and oxygen exposure. Additional well-established pharma excipients may also be able to enhance stability of dried vaccine material on VaxiPatches.

In summation, robust IgG responses were triggered as early as 2 weeks post-vaccination of naïve animals by QS-21 adjuvanted synthetic virosomes when delivered intradermally by VaxiPatch application. The scalable transient gene method is well suited for a seasonal or pandemic influenza context, in which the sequence of the target antigen changes frequently. However, this approach is highly modular, and could equally be pursued for other viral receptor glycoproteins such as the G protein of rabies, or the spike protein of SARS-CoV-2.

Recently, Kim et al., (2020) published a SAS-CoV-2 spike protein microneedle prototype COVID-19 vaccine [21]. We are also working on a SARS-CoV-2 spike protein COVID-19 vaccine using the methods described herein with the anticipation of building an automated GMP compliant manufacturing line.

This work serves as an initial characterization of the VaxiPatch system, specifically designed to be compatible with high-speed, efficient automated GMP manufacturing. VaxiPatch may allow for painless vaccination, with significant dose sparing, shipment at room temperature, and self-administration. This latter feature is of particular importance in epidemic or pandemic scenarios, in which there is significant risk associated with travel to hospitals and pharmacies to receive vaccinations. A self-applicable, thermostable skin patch could serve as a "shelter in place" vaccination strategy, in which vulnerable populations receive delivery at home without needing to engage an already-overtaxed health care infrastructure. All of these features could together increase the use of, and compliance with vaccines both in the US and abroad.

Declaration of Competing Interest

The authors declare that they have no known competing financial interests or personal relationships that could have appeared to influence the work reported in this paper.

Acknowledgements

We thank the UC Davis Venture Catalyst Program of which Verndari is a member. We thank the UC Davis Mouse Biology Program who performed the animal work. We thank Yeonju Song for early work on the VaxiPatch. This work was funded by Verndari, Inc.

Funding sources

This work was funded by Verndari Inc.

Author Contributors

TE designed and performed most of the lab work. GT and TE printed the microarray patches and GT performed many of the assays. DH conceived this work, designed and oversaw VaxiPatch fabrication, and directed the lab. DH and TE wrote the manuscript.

References

[1] Bloom DE, Fan VY, Sevilla JP. The broad socioeconomic benefits of vaccination. Sci Transl Med 2018;10.
[2] Orenstein WA, Ahmed R. Simply put: Vaccination saves lives. Proc Natl Acad Sci U S A 2017;114:4031–3.
[3] Francis Jr T. Vaccination against influenza. Bull World Health Organ 1953;8:725–41.
[4] Salk JE. Recent studies on immunization against poliomyelitis. Pediatrics 1953;12:471–82.
[5] Nelson KS, Janssen JM, Troy SB, Maldonado Y. Intradermal fractional dose inactivated polio vaccine: a review of the literature. Vaccine 2012;30:121–5.
[6] Zipprich J, Winter K, Hacker J, Xia D, Watt J, Harriman K, et al. Measles outbreak–California, December 2014-February 2015. MMWR Morb Mortal Wkly Rep 2015;64:153–4.
[7] Donnelly RF. Vaccine delivery systems. Hum Vaccin Immunother 2017;13:17–8.
[8] Taddio A, Ipp M, Thivakaran S, Jamal A, Parikh C, Smart S, et al. Survey of the prevalence of immunization non-compliance due to needle fears in children and adults. Vaccine 2012;30:4807–12.
[9] Arya J, Henry S, Kalluri H, McAllister DV, Pewin WP, Prausnitz MR. Tolerability, usability and acceptability of dissolving microneedle patch administration in human subjects. Biomaterials 2017;128:1–7.
[10] Littauer EQ, Mills LK, Brock N, Esser ES, Romanyuk A, Pulit-Penaloza JA, et al. Stable incorporation of GM-CSF into dissolvable microneedle patch improves skin vaccination against influenza. J Control Release 2018;276:1–16.
[11] Carter D, van Hoeven N, Baldwin S, Levin Y, Kochba E, Magill A, et al. The adjuvant GLA-AF enhances human intradermal vaccine responses. Sci Adv 2018. 4:eaas9930.
[12] Ameri M, Fan SC, Maa YF. Parathyroid hormone PTH(1–34) formulation that enables uniform coating on a novel transdermal microprojection delivery system. Pharm Res 2010;27:303–13.
[13] Peyraud N, Zehrung D, Jarrahian C, Frivold C, Orubu T, Giersing B. Potential use of microarray patches for vaccine delivery in low- and middle- income countries. Vaccine 2019;37:4427–34.
[14] Lee JW, Park JH, Prausnitz MR. Dissolving microneedles for transdermal drug delivery. Biomaterials 2008;29:2113–24.
[15] Park JH, Allen MG, Prausnitz MR. Biodegradable polymer microneedles: fabrication, mechanics and transdermal drug delivery. Conf Proc IEEE Eng Med Biol Soc 2004;4:2654–7.
[16] Park JH, Choi SO, Kamath R, Yoon YK, Allen MG, Prausnitz MR. Polymer particle-based micromolding to fabricate novel microstructures. Biomed Microdevices 2007;9:223–34.
[17] Christensen D. Vaccine adjuvants: Why and how. Hum Vaccin Immunother 2016;12:2709–11.
[18] Dunkle LM, Izikson R. Recombinant hemagglutinin influenza vaccine provides broader spectrum protection. Expert Rev Vaccines 2016;15:957–66.
[19] Spoulou V, Alain S, Gabutti G, Giaquinto C, Liese J, Martinon-Torres F, et al. Implementing Universal Varicella Vaccination in Europe: The Path Forward. Pediatr Infect Dis J 2019;38:181–8.
[20] Gabutti G, Bolognesi N, Sandri F, Florescu C, Stefanati A. Varicella zoster virus vaccines: an update. Immunotargets Ther 2019;8:15–28.
[21] Kim E, Erdos G, Huang S, Kenniston TW, Balmert SC, Carey CD, et al. Microneedle array delivered recombinant coronavirus vaccines: Immunogenicity and rapid translational development. EBioMedicine 2020;102743.